ELSEVIER

Journal of Power Sources 64 (1997) 13–19

JOURNAL OF POWER SOURCES

Influence of antimony on the properties of the anodic oxide layer formed on Pb–Sb alloys [1]

M. Metikoš-Huković [a], R. Babić [a], S. Brinić [b]

[a] *Department of Electrochemistry, Faculty of Chemical Engineering and Technology, University of Zagreb, Savska 16, PO Box 177, 10 000 Zagreb, Croatia*
[b] *Faculty of Technology, University of Split, N. Tesle 10, 21 000 Split, Croatia*

Abstract

Electric and dielectric properties, changes in structure and kinetics of formation and reduction of anodic phase layers on Pb and Pb–Sb electrodes in H_2SO_4 have been studied by means of electrochemical and structure characterizing impedance spectroscopy methods. The results obtained were discussed with respect to the effectiveness of Sb on the solid-state $PbO \rightarrow PbO_n$ and $PbO_n \rightarrow PbO_2$ transformations. It is found that Sb facilitates the appearance of a potential region in which non-stoichiometric mixed oxides are formed; it has a catalytic effect on the PbO into the PbO_n transformation. The formation of the mixed oxide leads to a shift in the potential of the oxidation of $PbSO_4$ to PbO_2 of about 200 mV in comparison with the pure-Pb electrode. It seems that the observed effects could explain why Sb prolongs the positive plate cycle life. It was shown that the electrochemical impedance spectroscopy is a very sensitive and suitable method for in situ investigation of solid-state processes in the positive lead/acid battery plate.

Keywords: Lead; Lead–antimony alloys; Lead/acid batteries; Impedance spectroscopy

1. Introduction

It has been established that antimony, widely used as an alloying additive in lead alloys for casting lead/acid battery grids, not only significantly affects the casting and mechanical properties of the alloys, but also has a strong impact on the electrochemical processes at the positive plate on the battery. Therefore, its influence on the electrochemical behaviour of Pb in Pb–Sb alloys in sulfuric acid solution has been extensively studied [1–18].

Antimony oxidation in Pb–Sb alloys begins at the potential values at which PbO formation takes place under the $PbSO_4$ perm-selective membrane [2–5]. It is believed that its oxidation in the alloy changes the composition of the anodic layer; simultaneously to the formation of lead oxide compounds (PbO, non-stoichiometric PbO_n and PbO_2), substituted $Pb_{(1-x)}Sb_xO$, non-stoichiometric $Pb_{(1-x)}Sb_xO_n$, and $Pb_{(1-x)}Sb_xO_2$ may be formed [9,18]. Since some of the above changes occur in the potential range where the lead/acid battery positive plate operates, they could probably explain the beneficial effect of Sb in a positive plate.

In our previous studies [19–21] the influence of Sb on the electrochemical behaviour on Pb–Sb alloys (1.3–3.5 wt.% Sb) in a solution of sulfuric acid, mostly in the potential range of PbO formation, was studied. In the present work, this study has been widened by investigating the electrochemical properties of the corrosion layer formed in the potential range above 1.20 V versus saturated calomel elctrode (SCE) in 0.5 M H_2SO_4 solution. Cyclic voltammetry and electrochemical impedance spectroscopy techniques have been used.

2. Experimental

The investigation was performed on pure-Pb (99.998 wt.%) and Pb–Sb alloys with an Sb content of 1.3, 2.7 and 3.5 wt.%, by means of cyclic voltammetry (CV) and electrochemical impedance spectroscopy (EIS). Scanning electron microscope (SEM) examination of the structure and morphology of Pb and Pb–Sb alloys was also carried out. The electrodes had a cylindrical form. The lateral surface of the cylinder was insulated by Araldite, exposing only the cylinder base plane to the solution; the surface area was 0.283 cm^2. Before each experiment, the electrodes were polished with silicon carbide grinding paper (grit 600), degreased in trichloroethylene, rinsed with distilled water, and, prior to each measurement, polarized for 10 min at −1.0 V, below the equilibrium potential of the $Pb/PbSO_4$ couple, to remove

[1] In memoria to Professor B. Lovreček.

PII S0378-7753(96)02494-9

oxides formed on the surface due to contact with air, and $PbSO_4$ formed during the immersion.

The experiments were performed in a standard two-compartment glass cell at 298 K using aqueous 0.5 M H_2SO_4 solution as the electrolyte. The counter electrode was a large platinum plate and the reference electrode was a SCE. All potential values in the paper are reported versus SCE.

Measurements were performed using an EG&G Princeton Applied Research Model 273 potentiostat, and an EG&G Model 5315 lock-in amplifier controlled by an IBM PC. Impedance measurements were performed in the frequency range 30 mHz to 100 kHz with the a.c. voltage amplitude ± 5 mV.

3. Results and discussion

3.1. Cyclic voltammetry on Pb–Sb alloys

Fig. 1 represents the current–potential curve for a Pb–Sb alloy with 2.7 wt.% Sb in a 0.5 M H_2SO_4 solution. Well-defined current maxima corresponding to oxidation and reduction processes of Pb, Sb and their compounds [2–5,19,20] can be seen. Almost the same voltammogram shape has been obtained on Pb–Sb alloys with an Sb content of 1.3 and 3.5 wt.%. A more detailed analysis of these voltammograms has been given in Refs. [19,20]. In short, the potential sweep in the positive direction first shows peak A_1 corresponding to formation of a $PbSO_4$ layer. Antimony oxidation (current peak A_s) begins in the PbO potential region under $PbSO_4$ perm-selective membrane. An increased anodic current above 1.8 V signifies both, oxidation of $PbSO_4$ to β-PbO_2, which is the stable phase in the acid solution, and an evolution of oxygen. The complexity of the voltammetric peaks on the early part of the reversed potential sweep is caused by simultaneous cathodic and anodic reactions that occur in this potential range. These are the PbO_2 discharge (peak C_3) and the oxidation of the Pb substrate and/or some

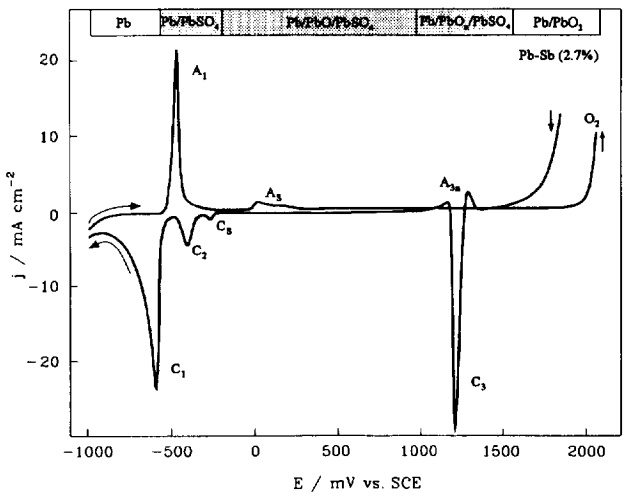

Fig. 1. Cyclic voltammogram on the Pb–2.7wt.%Sb electrode in 0.5 M H_2SO_4 solution; sweep rate 10 mV s^{-1}.

incompletely oxidized products of Pb. The current peak C_s corresponds to reduction of Sb(III) to Sb. Cathodic peak C_2, which appears at -0.47 V, corresponds to the reduction of tetra-PbO and basic lead sulfates. At potentials lower than -0.55 V, $PbSO_4$ reduction occurs, which is reflected in the cathodic peak C_1.

Antimony oxidation in the alloy changes the composition of the anodic layer. Pavlov and co-workers [9,18] proposed the formation of substituted Pb–Sb oxide species. Since their formation and reduction cannot be observed in the ordinary current–potential curve, a special procedure must be applied.

As usual, the pure-Pb electrode was used as a reference to which the results of the Pb–(1.3–3.5wt.%)Sb electrodes are compared. The disc electrodes, after treatment at -1.00 V, were subjected to a linear potential sweep (5 mV s^{-1}) up to a desired potential (above 1.20 V) at which they were oxidized at a constant potential for different periods of time. Then, a linear potential sweep of 5 mV s^{-1} in the cathodic direction was applied and the current–potential curve was registered.

The profile of the current–potential curve during the negative sweep is determined by the reduction processes that occur in the corrosion layer, and it can give evidence of the layer composition.

Fig. 2 represents the voltammograms of Pb and Pb–Sb electrodes, obtained after constant potential oxidation at 1.30, 1.40 and 1.60 V. Those parts of the voltammograms that represent the cathodic reduction of Pb and Pb–Sb higher oxides including non-stoichiometric ones are enlarged and represented in the insets to the diagrams. The main features of the voltammograms obtained for a Pb electrode are:

(i) The cathodic current maximum C_3, which represents the reduction of PbO_2, does not appear in the cyclic voltammogram after a prolonged anodic oxidation at 1.30 V. It does appear after oxidation at 1.40 V for 50 min.

(ii) The current maximum C_4, that begins to appear after a prolonged oxidation (240 min) at 1.20 V and is well expressed in the cyclic voltammogram obtained after oxidation at 1.30 V, corresponds to the reduction of the non-stoichiometric PbO_n. With increasing oxidation potential the cathodic peak C_4 increases.

However, when the process of PbO_2 formation starts and becomes the dominating one, the cathodic peak C_4 decreases.

Cyclic voltammograms of Pb–(1.3–3.5wt.%)Sb obtained by using the above procedure were almost identical in shape, and that is why we present only the voltammograms of a Pb–2.7wt.%Sb electrode. By comparing voltammograms of a Pb–2.7wt.%Sb electrode with those of a pure-Pb electrode, a few important differences can be observed:

(i) The amount of PbO_n (the current maximum C_4) in the anodic layer formed on the Pb–Sb electrode is higher than that in the anodic layer on a pure-Pb electrode.

(ii) The current maximum C_3 that corresponds to the reduction of PbO_2 in the corrosion layer appears after oxidation of alloys at 1.60 V. This potential is about 0.20 V

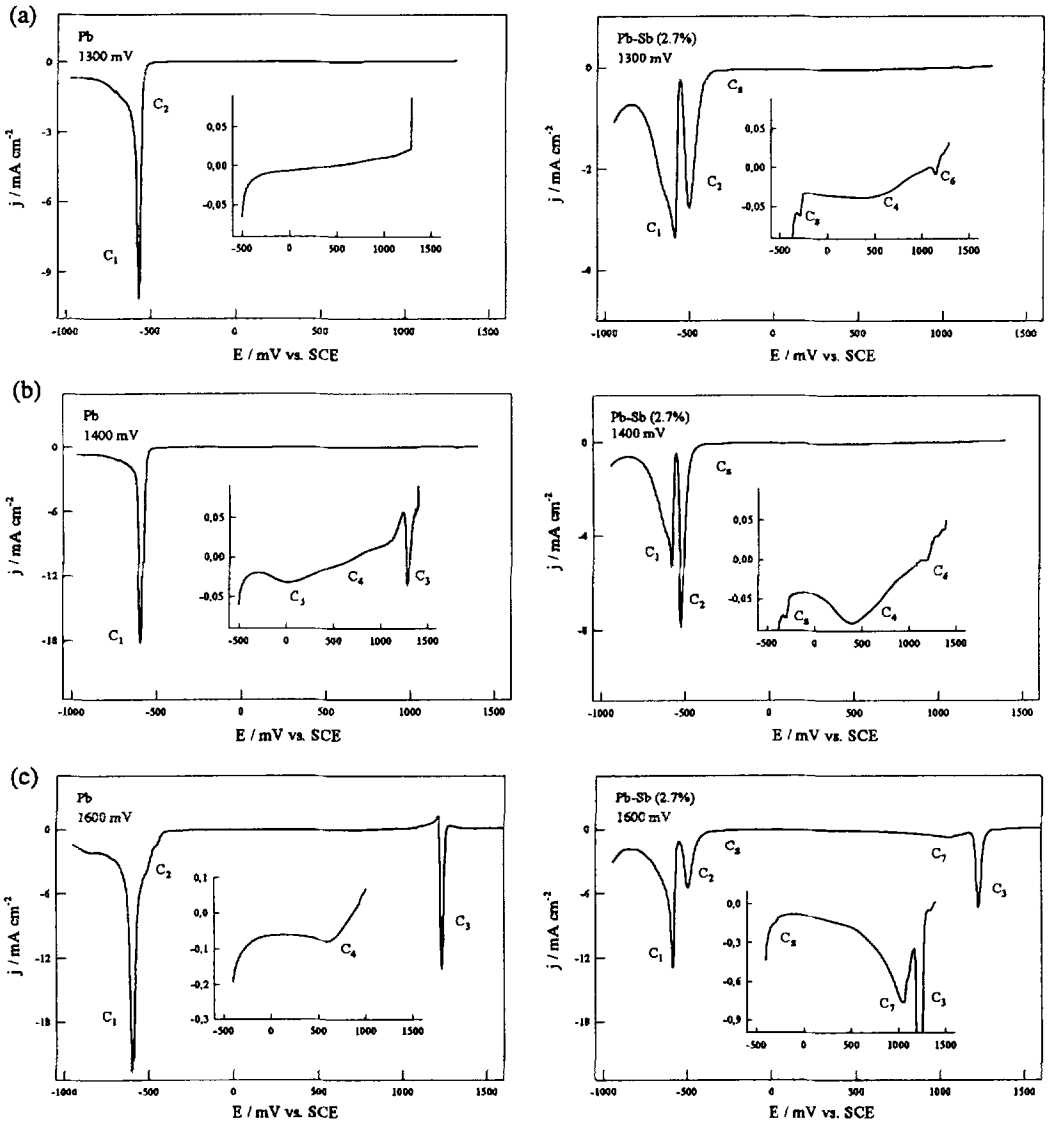

Fig. 2. Negative sweep voltammograms ($\nu = 5$ mV s^{-1}) on the Pb and Pb–2.7wt.%Sb electrode succeeding an oxidation for 50 min in 0.5 M H_2SO_4 at 1.30, 1.40 and 1.60 V, respectively.

higher than the potential at which PbO_2 can be formed on a pure-Pb electrode.

(iii) The new current peak C_6 (Fig. 2(a) and (b)) appears in the cyclic voltammograms obtained after oxidation of the Pb–Sb electrode at potentials between 1.30 and 1.50 V.

(iv) Cyclic voltammograms of Pb–(1.3–3.5wt.%)Sb alloys, after having been oxidized at 1.60 V, show also a current maximum C_7 (Fig. 2(c)).

In comparison with voltammograms of the Pb–12wt.%Sb electrode [9], it seems that the peak C_6 corresponds to a non-stoichiometric mixed oxide, e.g. $Pb_{(1-x)}Sb_xO_n$, while the current peak C_7 can be attributed to the formation of mixed $Pb_{(1-x)}Sb_xO_2$ oxide. The observed facts are in agreement with the data found by Pavlov et al. [18] that Sb facilitates the formation of non-stoichiometric oxides, PbO_n and $Pb_{(1-x)}Sb_xO_n$, and, at the same time, it retards the formation of PbO_2 in the corrosion layer. Voltammograms show that the amount of non-stoichiometric oxides PbO_n and $Pb_{(1-x)}Sb_xO_n$ depend on the amount of Sb in the alloy; the greater is the content of Sb in alloy, the higher is the amount of mixed oxides in the corrosion layer. Fig. 3 illustrates this statement. It represents cyclic voltammograms obtained when a pure-Pb electrode and Pb–(1.3–3.5wt.%)Sb electrodes were cathodically polarized after anodic oxidation at 1.30 V for 50 min. An increase in cathodic current proportional to the Sb content in alloy is obvious. It is possible to illustrate the above statement also by the potential decay curves; the potential decay curve on Pb shows only one potential arrest corresponding to reduction of PbO_n, while curves of Pb–Sb alloys show two arrests corresponding to reduction of both, $Pb_{(1-x)}Sb_xO_n$ and PbO_n.

The electrochemical behaviour of Pb–Sb alloys is investigated as a function of sweep rate in the potential range of PbO_2 formation and reduction (from 0.90 to 1.90 V). The results obtained were similar and those obtained for the Pb–1.3wt.%Sb electrode are presented in Fig. 4. Analysis of the peak currents and the peak potential dependence on a sweep rate ($\nu = 5$, 10, 20, 30 and 40 mV s^{-1}) [20] shows

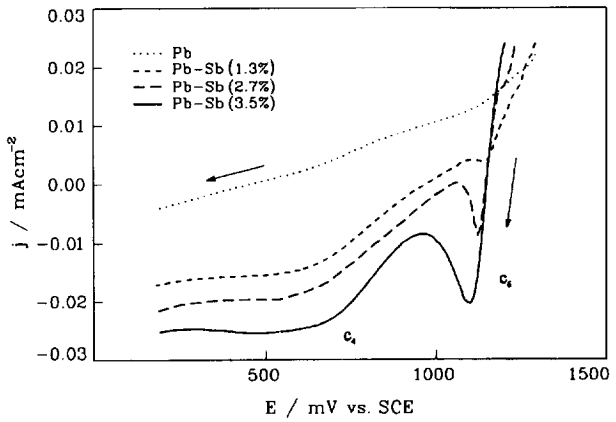

Fig. 3. Negative sweep voltammograms ($\nu = 5$ mV s^{-1}) on the Pb and Pb–(1.3, 2.7 and 3.5 wt.%)Sb electrodes succeeding an oxidation for 50 min at 1.30 V in 0.5 M H_2SO_4.

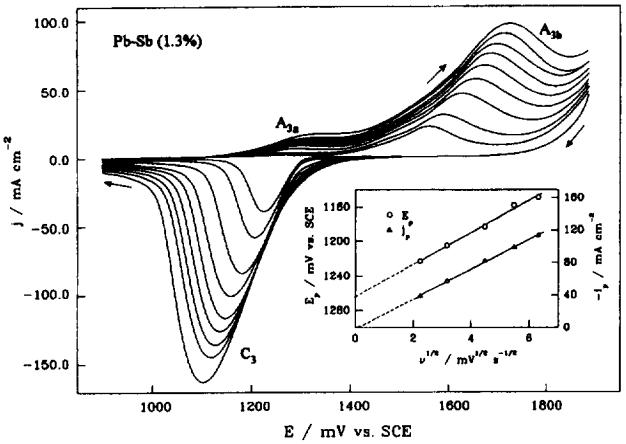

Fig. 4. Cyclic voltammograms on the Pb–1.3wt.%Sb electrode in 0.5 M H_2SO_4 solution; $\nu = 5$, 10, 20, 30, 40, 50, 60, 70 and 100 mV s^{-1}.

that the potential-determining reaction occurring at the cathodic peak corresponds to the reduction of β-PbO_2 which is under ohmic resistance control. The inset to Fig. 4 shows the linear relationship between the peak current, I_p, and the peak potential, E_p versus the square root of the sweep rate, respectively. The value of the ohmic resistance calculated as dE/dI amounted to 1.05 Ω. A very good agreement can be observed in comparison with the resistance obtained at the same potential by the impedance method. A linear relationship is observed between the potential peak potential, E_p and $\nu^{1/2}$ which, when extrapolated to the zero scan rate, gives a spontaneous redox potential $E(\nu = 0)$. The absence of the polarization effect makes these the most suitable values for comparison with thermodynamic data. The difference between experimental value $E_0 = 1.27$ V and $E_{rev}(PbO_2/PbSO_4) = 1.38$ V gives the cathodic nucleation overpotential $\eta_{cn} = E_0 - E_{rev} = -0.11$ V. A good agreement between the extrapolated potential value and the thermodynamic one indicates that the reactive electrochemical form of lead dioxide is formed, since its less reactive (chemically prepared) form cannot be reduced to lead sulfate [22].

3.2. Electrochemical impedance spectroscopy data

In order to investigate how the apparent formation of Pb–Sb non-stoichiometric oxides could influence the electrical conductivity of the anodic-phase layer, EIS measurements were performed for both the pure-Pb and the Pb–Sb electrodes after they have been oxidized at different potentials in the potential range between 1.20 and 1.40 V. The results obtained are presented in a Bode plot in Figs. 5 and 6, together with the corresponding equivalent circuit which has given the best fitting procedure of the experimental data. Since the results obtained on Pb–Sb alloys were similar, only those obtained for the Pb–2.7wt.%Sb electrode are presented in Fig. 6.

The equivalent circuit consists of serial combination of two subcircuits. The first one can be associated with transformation of PbO into non-stoichiometric oxides, and the second one which process takes place between the anodic layer and the solution. The constant phase elements Q_1 and Q_2

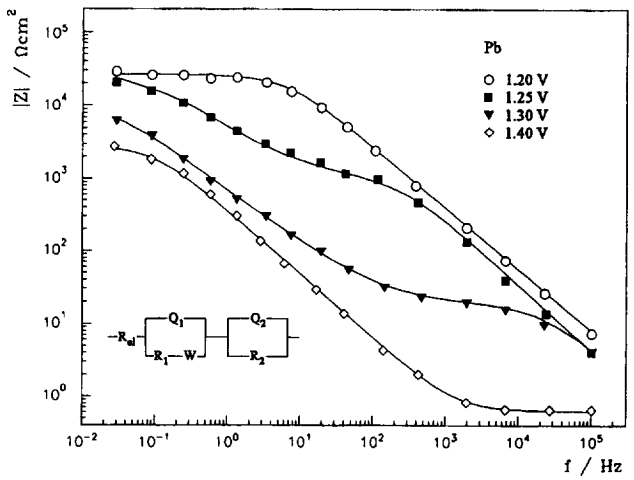

Fig. 5. Bode plots for the Pb electrode at: (○) 1.20; (■) 1.25; (▼) 1.30 and (◇) 1.40 V after 50 min of polarization.

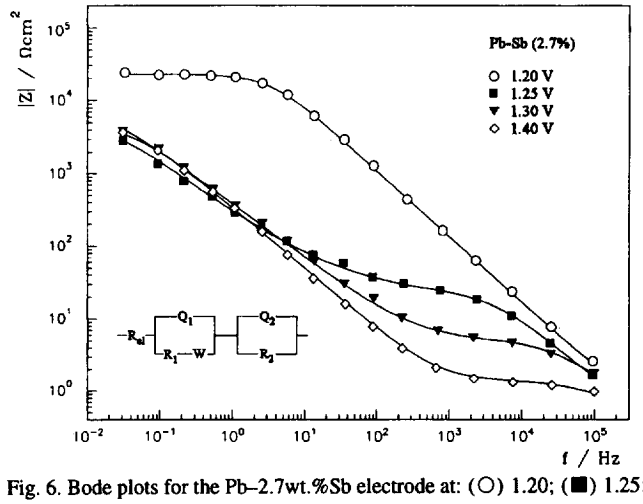

Fig. 6. Bode plots for the Pb–2.7wt.%Sb electrode at: (○) 1.20; (■) 1.25; (▼) 1.30 and (◇) 1.40 V after 50 min of polarization.

Table 1
Fit parameters for a Pb electrode oxidized in 0.5 M H_2SO_4 for 50 min at different potentials

Potential (V)	1.200	1.250	1.275	1.300	1.400
R_{el} (Ω cm^2)	0.7	0.5	0.6	0.5	0.6
Q_1 (Ω^{-1} cm^{-2} s^n $\times 10^{-6}$)	1.50	1.30	2.45	2.40	
n	0.861	0.921	0.871	0.869	
R_1 (Ω cm^2)	26340	897	33.0	16.9	
W (Ω^{-1} cm^{-2} s$^{0.5}$ $\times 10^{-3}$)		0.14	2.60	3.4	
Q_2 (Ω^{-1} cm^{-2} s^n $\times 10^{-6}$)		99.0	323	401	547
n		0.892	0.772	0.796	0.889
R_2 (Ω cm^2)		7949	13900	9777	2794

Table 2
Fit parameters for a Pb–2.7wt.%Sb electrode oxidized in 0.5 M H_2SO_4 for 50 min at different potentials

Potential (V)	1.200	1.250	1.275	1.300	1.400
R_{el} (Ω cm^2)	0.7	0.4	0.7	0.7	0.6
Q_1 (Ω^{-1} cm^{-2} s^n $\times 10^{-6}$)	2.65	5.9	12.5	7.0	39
n	0.907	0.877	0.827	0.867	0.81
R_1 (Ω cm^2)	23536	22.0	5.7	4.08	0.9
W (Ω^{-1} cm^{-2} s$^{0.5}$ $\times 10^{-3}$)		2.50	9.70	16.1	
Q_2 (Ω^{-1} cm^{-2} s^n $\times 10^{-6}$)		1369	1484	668	575
n		0.864	0.797	0.768	0.856
R_2 (Ω cm^2)		2993	3962	9101	5401

$$Z_{cpe} = Q(j\omega)^{n-1} \quad (1)$$

have been taken rather than pure capacitance elements because of better fit results. The Warburg-like diffusion component Z_w must be related to a process under diffusion control through a finite region of the anodic layer [23]. The values of the equivalent circuit parameters for Pb and Pb–2.7wt.%Sb electrodes are presented in Tables 1 and 2, respectively.

After 50 min of oxidation at 1.20 V the impedance spectra of Pb and Pb–2.7wt.%Sb alloy have similar shapes with only one time constant R_1Q_1, where R_1 is the resistance of the PbO layer inside the $PbSO_4$ membrane and Q_1 represents its dielectric properties. With increasing oxidation potential, impedance spectra exhibit a capacitive contribution at higher frequencies and an indication of a second time constant at lower frequencies. The time constant at higher frequencies diminishes gradually with increasing potential of oxidation.

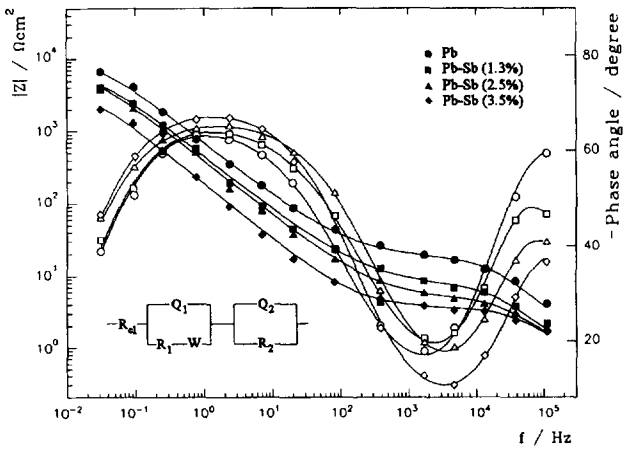

Fig. 7. Bode plots for (●) the Pb and Pb–Sb electrodes: (■) 1.3; (▲) 2.7, and (◆) 3.5 wt.% Sb at 1.30 V after 50 min of polarization.

The influence of the Sb content in Pb–Sb alloys on the impedance spectra recorded, after the electrodes have been oxidized for 50 min at 1.30 V, can be seen in Fig. 7. Values of resistance R_1 can be taken as a probe for the d.c. conductivity of the layer. Its dependence on the oxidation potential and the Sb content is illustrated in Fig. 8.

A stronger decrease in resistance of the anodic-phase layer on Pb–Sb alloys with increasing potential than on a pure-Pb electrode is obvious. At 1.40 V, as can be seen from Tables 1 and 2, the resistance R_1 disappears in the anodic layer on a Pb electrode, while it is still present in the anodic layer on the Pb–Sb electrode. This is obviously a consequence of a new phase formed in the anodic layer on Pb–Sb electrodes which have been detected by voltammetric measurements (peak C_6 on Fig. 2). Hence, the impedance measurements confirm that the presence of Sb in Pb–Sb alloys favours the solid-state oxidation of Pb(II) into non-stoichiometric Pb and

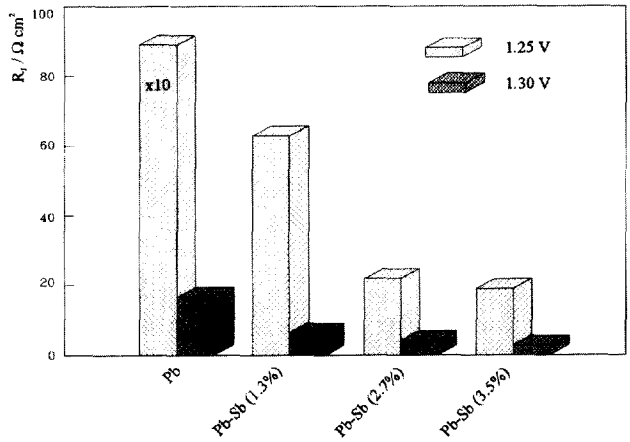

Fig. 8. Layer resistance R_1 vs. Sb content.

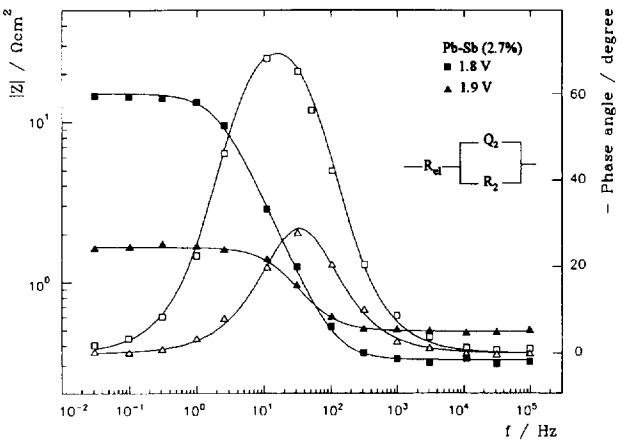

Fig. 9. Bode plots for the Pb–2.7wt.%Sb electrode in 0.5 M H_2SO_4 at (■) 1.80 V, and (▲) 1.90 V.

a mixed lead oxide in the anodic layer, and increases its conductivity. Thus, Sb may act as a solid-state catalyst for Pb(II) oxidation as noted by Pavlov et al. [9]. Formation of the relatively conductive non-stoichiometric oxides and their stability at potentials more negative than the equilibrium one for $PbO_2/PbSO_4$ electrode may influence the capacity of the positive lead/acid battery plate [18]. During discharge, the $Pb_{(1-x)}Sb_xO_n$ oxide preserves the electronic contact between the grid and positive active material of the plate down the more negative potentials before the high ohmic PbO layer is formed and the plate is strongly polarized.

Impedance measurements confirm also cyclic voltammetry findings that Sb retards the anodic oxidation of $PbSO_4$ into PbO_2.

Fig. 9 represents impedance spectra obtained on the Pb–2.7wt.%Sb electrode at 1.80 and 1.90 V together with the corresponding equivalent circuit. This consists of only one time constant $R_{ct}Q_{dl}$, where R_{ct} represents the kinetic resistance, i.e. the charge-transfer resistance of oxygen evolution [24]

$$R_{ct} = \lim_{\omega \to 0} Re\{Z_f\} \quad (2)$$

The graph shows that R_{ct} decreases with increasing anodic polarization. Since the oxygen evolution reaction can occur only on the β-PbO_2 layer that acts as a degenerate semiconductor with metallic properties [25,26]. By increasing its content in the phase layer the rate of oxygen evolution increases too, i.e. the charge-transfer resistance decreases.

4. Conclusions

The electrochemical behaviour of Pb and Pb–Sb binary alloys with an Sb content of 1.3 to 3.5% was studied in the potential region above 1.20 V versus SCE. The investigation was performed in 0.5 M H_2SO_4 solution by means of cyclic voltammetry and electrochemical impedance spectroscopy techniques.

During anodic polarization of the Pb–Sb electrodes the semipermeable $PbSO_4$ layer forms first, and then underneath it, depending on the electrode potential, several processes occur resulting in the formation of PbO and the substituted lead–antimony oxide $Pb_{(1-x)}Sb_xO$, then non-stoichiometric PbO_n and the mixed $Pb_{(1-x)}Sb_xO_n$ $(1<n<2)$, and finally PbO_2 and the mixed $Pb_{(1-x)}Sb_xO_2$.

It is found that Sb facilitates the appearance of a potential region (about 50 mV) in which non-stoichiometric $Pb_{(1-x)}Sb_xO_n$ is formed; it has a catalytic effect on PbO into PbO_n transformation. The formation of the mixed oxide leads to a shift in the potential of oxidation of $PbSO_4$ to PbO_2 of about 200 mV in comparison with the pure-Pb electrode. It seems that the observed effects could explain why Sb prolongs positive plate cycle life.

It was shown that impedance spectroscopy in combination with cyclic voltammetry is a very sensitive and suitable method for in situ investigation of solid-state processes in the positive lead/acid battery plate.

5. List of symbols

CPE	constant-phase element
E	potential, V
I	current, A
n	constant-phase element exponent
Q	constant-phase element coefficient, Ω^{-1} s^n
R	resistance, Ω
W	Warburg impedance, Ω^{-1} $s^{0.5}$
Z	impedance, Ω

Greek letters

η	overpotential
ν	scan rate, V s^{-1}
ω	angular frequency, rad^{-1}

Subscripts/superscripts

cd	cathodic nucleation
ct	charge transfer
dl	double layer
f	faradaic
p	peak

References

[1] S. Laihonen, T. Laitinen, G. Sundholm and A. Yli-Pentti, *Electrochim. Acta, 35* (1990) 229.
[2] H.S. Panesar, in D.H. Collins (ed.), *Power Sources 3*, Oriel Press, Newcastle-upon-Tyne, 1971, p. 79.
[3] T.F. Sharpe, *J. Electrochem. Soc., 124* (1977) 168.
[4] J.C. Chang, M.M. Wright and E.M.L. Valeriste, in D.H. Collins (ed.), *Power Sources 6*, Academic Press, New York, 1977, p. 69.
[5] B.K. Mahato, *J. Electrochem. Soc., 126* (1979) 365.
[6] J.S. Buchanan and L.M. Peter, *Electrochim. Acta, 33* (1988) 127.
[7] P. Ruetschi, *J. Electrochem. Soc., 120* (1973) 331.

[8] P. Ruetschi and B.D. Cahan, *J. Electrochem. Soc., 105* (1958) 369.
[9] D. Pavlov, B. Monahov, G. Sundholm and T. Laitinen, *J. Electroanal. Chem., 305* (1991) 57.
[10] D. Pavlov and B. Monahov, *J. Electroanal. Chem., 218* (1987) 135.
[11] N.A. Hampson, S. Kelly and K. Peters, *J. Appl. Electrochem., 10* (1980) 91.
[12] A.G. Gaad Allah, H.A.A. El-Rahman, S.A. Salih and M.A. El-Galil, *J. Appl. Electrochem., 22* (1992) 571.
[13] M.P.J. Brennan, B.N. Stirrup and N.A. Hampson, *J. Appl. Electrochem., 4* (1974) 497.
[14] J.A. Bialacki, N.A. Hampson and F. Wilson, *J. Appl. Electrochem., 15* (1985) 99.
[15] T. Rogatchev, St. Ruevski and D. Pavlov, *J. Appl. Electrochem., 6* (1976) 33.
[16] T. Laitinen, K. Salmi, G. Sundholm, B. Monahov and D. Pavlov, *Electrochim. Acta, 36* (1991) 605, and Refs. therein.
[17] M.N. Ijomah, *J. Electrochem. Soc., 134*y (1987) 1960.
[18] B. Monahov and D. Pavlov, *J. Electrochem. Soc., 141* (1994) 2316.
[19] R. Babić, M. Metikoš-Huković, N. Lajqy and S. Brinić, *J. Power Sources, 52* (1994) 17.
[20] M. Metikoš-Huković, R. Babić and S. Omanović, *J. Electroanal. Chem., 347* (1994) 199.
[21] S. Brinić, M. Metikoš-Huković and R. Babić, *J. Power Sources, 55* (1995) 19.
[22] S.M. Caulder, J.S. Murday and A.C. Simon, *J. Electrochem. Soc., 120* (1973) 1515.
[23] F.E. Varela, L.M. Gassa and J.R. Vilche, *J. Electroanal. Chem., 353* (1993) 147.
[24] W.J. Lorentz and F. Mansfeld, *Corr. Sci., 21* (1981) 647.
[25] J.S. Buchanan, N.P. Freestone and L.M. Peter, *J. Electroanal. Chem., 182* (1985) 383.
[26] J.S. Buchanan and L.M. Peter, *Electrochim. Acta, 33* (1988) 127.